Design Parameters for Superhydrophobicity and Superoleophobicity

Anish Tuteja, Wonjae Choi, Gareth H. McKinley, Robert E. Cohen, and Michael F. Rubner

Abstract

Recent experiments have revealed that the wax on the lotus leaf surface, by itself, is weakly hydrophilic, even though the lotus leaf is known to be superhydrophobic. Conventional understanding suggests that a surface of such waxy composition should not be able to support superhydrophobicity and high contact angles between a liquid and the surface. Here, we show that the unexpected superhydrophobicity is related to the presence of "reentrant texture" (that is, a multivalued surface topography) on the surface of the lotus leaf. We exploit this understanding to enable the development of superoleophobic surfaces (i.e., surfaces that repel extremely low-surface-tension liquids, such as various alkanes), where essentially no naturally oleophobic materials exist. We also develop general design parameters that enable the evaluation of the robustness of the composite interface on a particular surface. Based on these design parameters, we also rank various superhydrophobic and superoleophobic substrates discussed in the literature, with particular emphasis on surfaces developed from inherently hydrophilic or oleophilic materials.

Introduction

The most widely known example of a natural superhydrophobic surface is the surface of the lotus leaf (*Nelumbo nucifera*). Numerous studies have suggested that the combination of surface chemistry and roughness on multiple scales[1–4] on the lotus leaf's surface (see the inset of Figure 1a) allows for the trapping of microscopic pockets of air underneath a water droplet. This trapped air imbues the leaf with its characteristic superhydrophobicity (see Figure 1a). However, a liquid with a markedly lower surface tension such as hexadecane (γ_{lv} = 27.5 mN/m) rapidly wets the lotus surface, leading to a contact angle of ~0° (see Figure 1b), clearly demonstrating the leaf's oleophilicity. Indeed, despite the plethora of superhydrophobic surfaces, there are no naturally occurring superoleophobic surfaces.[5–11] Here, we define superoleophobic surfaces as those that display contact angles greater than 150° with organic liquids such as alkanes, which have appreciably lower surface tensions than water.

In the present work, we describe the development of surface textures that resist wetting by a wide range of liquids, through the systematic control of their surface energy and topography. Examples of the coatings developed using this approach are shown in Figures 1c and 1d. These images show how a specially designed polymeric coating is used to confer oleophobicity, in addition to superhydrophobicity, to a lotus leaf.

Biomimetic Wettability

The surfaces of numerous plants and insects have wetting properties that inspire the development of analogous engineered materials. The engineering of surfaces that, mimicking the lotus leaf, have both high apparent contact angles and low roll-off angles with any liquid requires the formation of a composite interface and the trapping of air underneath the liquid droplet.[12] Air entrapment through superhydrophobic rough textures is also used by several aquatic insects to provide an oxygen–carbon dioxide exchange space, commonly referred to as a "plastron."[13]

Zhai et al.[14] recently demonstrated that it is possible to mimic the superhydrophobicity of the lotus leaf surface by creating a honeycomblike hydrophobized polyelectrolyte multilayer surface coated with silica nanoparticles (Figure 1e). The inset of Figure 1e shows an image of this superhydrophobic polyelectrolyte multilayer surface submerged in a pool of water. The submerged surface acts like a mirror when viewed at a critical angle,[15] displaying reflections of objects placed in front of it. The reflective surfaces visible underneath the liquid droplets in Figures 1a, 1c, and 1d similarly confirm the presence of a composite liquid–vapor interface.

In more recent work, Zhai et al. showed[16] that it is also possible to mimic the water-harvesting surface characteristics of the wings of the desert Namib beetle. This was achieved by creating hydrophilic and superhydrophilic[17] (with water contact angle ≈ 0°) patterns on superhydrophobic surfaces, as shown in Figure 1f. The experimental scheme used to produce these surfaces provides a general approach for generating patterned surfaces that can be used to control the confinement of water droplets, thereby producing channels on surfaces.

Surface Roughness and Apparent Contact Angles

The engineering of liquid-repellent surfaces typically involves the manipulation of two key surface parameters: surface energy and roughness.[2,18–21] The overall free energy of the system determines whether a given liquid fully wets or creates a composite interface with a particular textured surface.[20–23] In contrast to a fully wetted interface, the composite interface typically leads to high contact angles and low roll-off angles (corresponding to low contact-angle hysteresis).[2,5,24]

Studies show that a series of rough or textured substrates with progressively decreasing surface energy, or increasing equilibrium contact angles (θ), exhibit a transition from a fully wetted state to a composite interface.[24–26] Equating the Cassie[19] and Wenzel[18] relations gives the critical value of the equilibrium contact angle (θ_c)[27] for this transition. Contact angles above θ_c lead to a lower overall free energy for the composite interface than for the corresponding fully wetted interface

$$\cos\theta_c = \frac{(\phi_s - 1)}{(r - \phi_s)}. \quad (1)$$

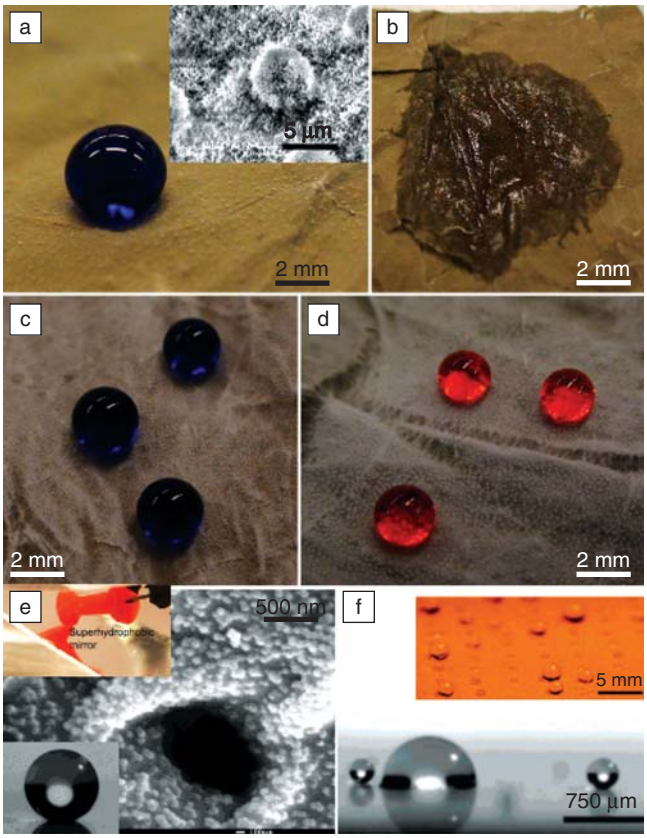

Figure 1. (a) Droplet of water (colored with methylene blue) on a lotus leaf surface. The leaf's surface is textured with small (10–20 μm) protruding nubs, which are further covered with nanometer-size epicuticular wax crystalloids. The inset shows a scanning electron microscopy (SEM) image of the lotus leaf surface. (b) Wetted surface of the lotus leaf after contact with a droplet of hexadecane. (c), (d) Droplets of (c) water (colored with methylene blue) and (d) hexadecane (colored with Oil Red O) on a lotus leaf surface covered with electrospun fibers of poly(methyl methacrylate) (PMMA) + 44 wt% fluoroPOSS (fluorinated polyhedral oligomeric silsesquioxane). A reflective surface is visible under the droplets in both images, indicating the presence of microscopic pockets of air. [Reproduced with permission from Reference 6. Copyright 2007 American Association for the Advancement of Science (AAAS).] (e) Honeycomblike structure of a superhydrophobic polyelectrolyte multilayer film coated with silica nanoparticles. [Reproduced with permission from Reference 14. Copyright 2004 American Chemical Society (ACS).] The insets show a droplet of water sitting on the aforementioned surface and an optical image of a glass slide coated with the superhydrophobic polyelectrolyte multilayer surface submerged in a pool of water. (f) Optical micrograph showing small water droplets sprayed on a superhydrophobic surface with an array of hydrophilic domains patterned using a 1% poly(acrylic acid) water/2-propanol solution. (Reproduced with permission from Reference 16. Copyright 2006 ACS.)

Here, r is the surface roughness,[18] and ϕ_s is the fraction of the solid in contact with the liquid.[19] From previous discussions,[6] it is apparent that $r > 1 > \phi_s$. Hence, for any given surface, Equation 1 predicts that $\cos\theta_c < 0$ or $\theta_c > 90°$. Thus, it can be anticipated that that the creation of highly nonwetting surfaces (apparent contact angles $\theta^* >> 90°$) with low hysteresis requires equilibrium contact angles to be in the range $\theta > \theta_c > 90°$. These arguments highlight the difficulty of developing surfaces that repel alkanes such as decane or octane, as there are no reports of natural or artificial surfaces with low enough surface energy to enable equilibrium contact angles of $\theta > 90°$ with these liquids.[6–9,11]

The Effects of Reentrant Texture

Recent studies have shown that the wax on the surface of the lotus leaf is weakly hydrophilic ($\theta \approx 74°$).[28] From the preceding discussions in this article, it would be expected then that water should fully wet the lotus leaf surface and thus lead to apparent contact angles $\theta^* << 90°$, as predicted by the Wenzel relation.[18] Herminghaus[12] first pointed out that the various surface constituents of the leaves of a number of superhydrophobic plants, such as the common smoketree (*Cotinus coggygria*) or wild cabbage (*Brassica oleracea*), are hydrophilic. The surprising superhydrophobicity of such plant leaves is expected to be a consequence of reentrant surface texture;[3,6,10,12,29] that is, the surface topography cannot be described by a simple univalued function $z = h(x,y)$, and a vector projected normal to the x–y plane intersects the texture more than once.

Consider the schematics shown in Figures 2a and 2b, which depict imaginary solid–liquid–vapor profiles for a hypothetical liquid with $\theta \approx 70°$ on two different surfaces. If $\theta < \psi$, the local texture angle, as in Figure 2a, the net traction on the liquid–vapor interface is downward, thereby facilitating the imbibition of the liquid into the solid structure, leading to a fully wetted interface. On the other hand, if $\theta > \psi$, as shown in Figure 2b, the net traction is directed upward, thereby supporting the formation of a composite interface.[3] In other words, either of these surfaces can support the formation of a composite interface provided that $\theta > \psi$,[6,20,21] and any liquid for which $\theta < \psi$ will immediately yield a fully wetted interface.

The presence of reentrant texture (or $\psi < 90°$) in the surface illustrated in Figure 2b allows for the formation of a composite interface and thus extremely high apparent contact angles even if $\theta < 90°$. Recently, Cao et al.[3] used this idea to develop silicon micropost arrays with reentrant texture (Figure 2c) that exhibited superhydrophobicity, even though the equilibrium contact angle for water on the flat silicon surface was $\theta = 74°$.

In further studies of reentrant texture, Nosonovsky[21] analyzed the stability of composite interfaces on surfaces having different roughness profiles. He argued that the creation of a stable composite interface on any rough surface requires two criteria to be satisfied. One is that there must exist a local texture angle (ψ) equal to the equilibrium contact angle θ. The second condition states that, in the vicinity of the local region where $\theta = \psi$, the differential quantities related to changes in the solid–liquid contact area (dA_{sl}) and the local contact angle ($d\theta$) with the advancing or receding of the liquid have opposite signs such that $dA_{sl}d\theta < 0$.

Based on these criteria, Nosonovsky proposed a liquid-repellent structure of rectangular pillars, covered with semicircular ridges and grooves as shown in Figure 2d. Because of the presence of reentrant curvature at several locations on this structure

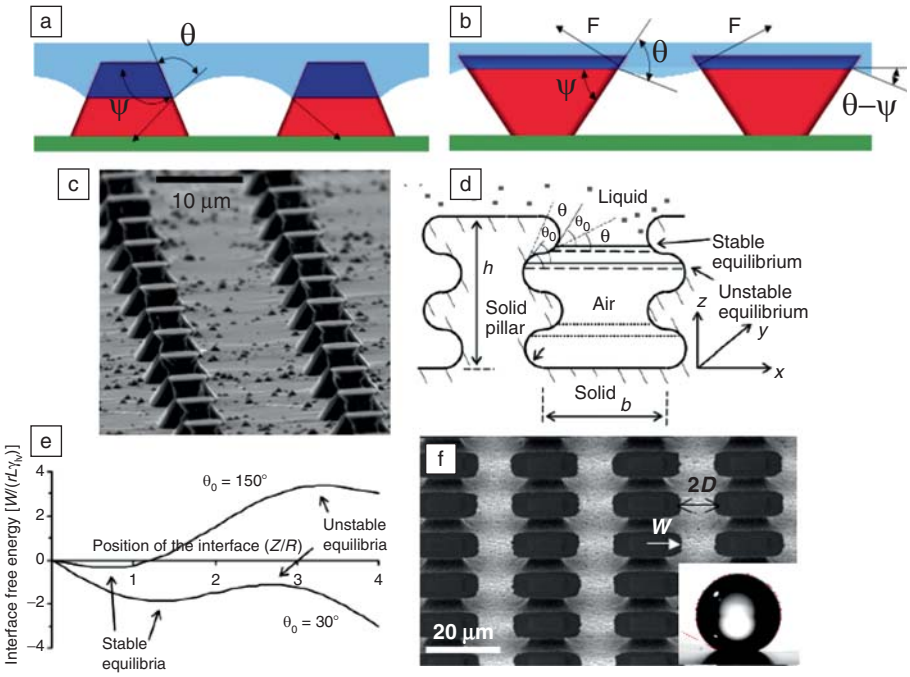

Figure 2. (a), (b) Schematic diagrams illustrating the expected liquid–vapor interface on two idealized surfaces with different values of the equilibrium contact angle (θ). The liquid is light blue. Air is white. The dark blue surface is wetted, whereas the red surface is nonwetted. (c) Silicon micropost arrays developed by Cao et al.[3] (Reproduced with permission. Copyright 2007 ACS.) (d) Schematic of a surface exhibiting reentrant curvature proposed by Nosonovsky.[21] The height of the pillars is h; b is inter-pillar spacing. (Reproduced with permission from Reference 21. Copyright 2007 ACS.) (e) Computed overall free energy as a function of the penetration depth (z) for two cases, one in which the surface shown in Figure 2d is considered to be extremely hydrophobic (θ = 150°) and one in which the surface is considered to be hydrophilic (θ = 30°). A local minimum in free energy leads to an energetically stable droplet configuration (composite or fully wetted), whereas a local maximum is unstable. (Reproduced with permission from Reference 21. Copyright 2007 ACS.) (f) Scanning electron micrograph of the micro-hoodoo surface. The inset shows a droplet of octane with θ* = 155° on the micro-hoodoo surface. (Reproduced with permission from Reference 6. Copyright 2007 AAAS).

(where 0° < ψ < 90°), such a surface provides the possibility of obtaining a composite interface with any liquid for which θ > 0°.[6] Figure 2e shows the computed free energy as a function of the penetration depth of the liquid–vapor interface (z), for hydrophilic (θ = 30°) and hydrophobic (θ = 150°) surfaces having the same texture as shown in Figure 2d. It can be seen that it is possible to form a composite interface (for $z \approx 1.5$) on the hydrophilic surface (leading to extremely high apparent contact angles), even though the equilibrium contact angle for this surface is only 30°. However, this composite interface configuration is not the true equilibrium state, as the fully wetted interface (for $z \approx 4$) leads to a lower overall free energy. Nonetheless, it is clear that the correct choice of surface texture can lead to the formation of "metastable" (energetically trapped) composite interfaces[3,6,10,12,23] and extremely high apparent contact angles, even though the solid surface by itself might be hydrophilic. Given these considerations, it might similarly be possible to develop superoleophobic surfaces, even though the candidate substrates are limited to solid materials with θ < 90° for various low-surface-energy alkanes.

Motivated by this theoretical understanding, our group at Massachusetts Institute of Technology (MIT)[6] fabricated model structures with reentrant curvature, of the form shown in Figure 2f. These structures were fabricated on flat Si wafers using SiO_2 deposition, followed by a two-step etching process that results in undercut silicon pillars (covered with a 300-nm layer of SiO_2) and troughs.[6] We refer to these structures as micro-hoodoos. The name arises from the fact that the topography and fabrication process of these structures are similar to those of naturally occurring geomorphological features called hoodoos that are created by soil erosion. Hoodoos are composed of a soft sedimentary rock topped by a piece of harder, less easily eroded stone.

The inset of Figure 2f shows the shape of a droplet of octane on the micro-hoodoo surfaces. Contact angles as high as θ* = 163° were observed with heptane, octane, and decane, and a 10 μl drop of octane could be easily rolled off this surface by tilting it to 15°. Krupenkin et al. also recently described model surfaces with reentrant curvature termed nanonails in an effort to develop superoleophobic surfaces based on similar ideas.[10]

Another example of a textured surface featuring reentrant curvature is a nonwoven mat of electrospun[31–33] fibers formed from a blend of a hydrophilic polymer [poly(methyl methacrylate), PMMA] and the extremely low-surface-energy molecule fluoroPOSS (fluorinated polyhedral oligomeric silsesquioxanes).[6] See the inset of Figure 3a. The complex reentrant topography allows for the establishment of stable composite interfaces with various liquids, including water and alkanes such as octane. This enables the surface to display extremely high apparent contact angles, even though the constituent fibers themselves are hydrophilic and oleophilic, respectively.[6,32]

This effect is further explored in the form of a general wetting diagram as shown in Figure 3a. The apparent advancing (θ^*_{adv}) and receding (θ^*_{rec}) contact angles for water on the rough electrospun surfaces for various PMMA/fluoroPOSS blend concentrations are plotted as a function of the corresponding advancing and receding contact angles on smooth (spin-coated) surfaces. By increasing the mass fraction of the fluoroPOSS molecules blended with PMMA, it is possible to systematically lower the surface tension for the polymer–fluoroPOSS blend, thereby allowing access to this entire parameter space with a single liquid (water). It can be seen from the figure that a few data points lie in the lower right quadrant (IV) of this diagram. These surfaces correspond to hydrophilic substrates that are rendered hydrophobic purely by reentrant topography.

To further elucidate the significance of reentrant curvature in the formation of a metastable composite interface, our group at MIT calculated[6] the variation in the specific Gibbs free energy arising from the progressive penetration of the liquid–air interface into various textured surfaces. These calculations were based on the formulation described by Marmur,[20] and details of our calculations can be found in the cited work.[6]

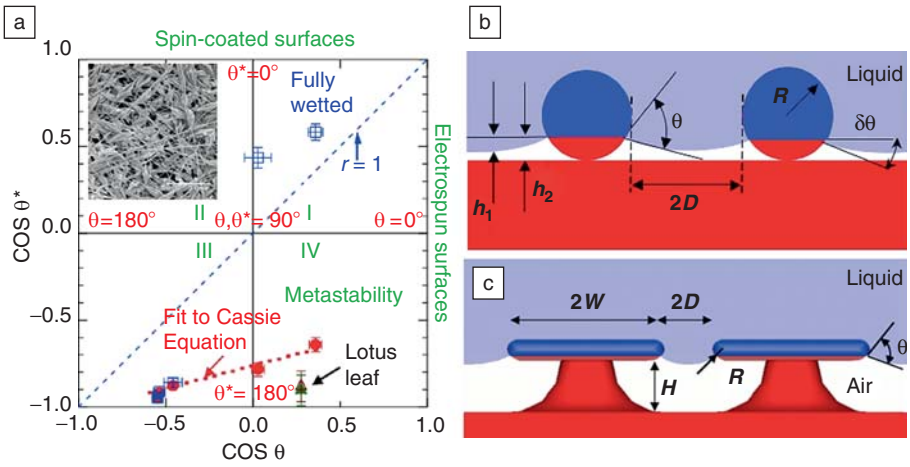

Figure 3. (a) cos θ^*_{adv} (where θ^*_{adv} is the advancing angle on the reentrant elecrospun surface, red circles) and cos θ^*_{rec} (where θ^*_{rec} is the receding angle on the reentrant electrospun surface, blue squares) for water as functions of cos θ_{adv} and cos θ_{rec}. Experiments show that water droplets released from a sufficiently large height can penetrate and wet the fiber mats that lie in quadrant IV, confirming the metastability of the composite interface on these surfaces. The advancing and receding contact angles for a lotus leaf are also provided for comparison. The inset shows an SEM image for an electrospun surface composed of PMMA + 9.1 wt% fluoroPOSS. (Reproduced with permission from Reference 6. Copyright 2007 AAAS.) (b) Schematic of the electrospun fibers, illustrating their idealized configuration. (c) Schematic illustrating the important topographic features of the micro-hoodoo surface.

As an introductory example, our group at MIT calculated the Gibbs free energy density variation for water (Figure 4a; $\theta = 120°$) penetrating into a surface covered with sinusoidal wrinkles (see the inset of Figure 4a). It can be seen from Figure 4a that, for water on the hydrophobic surface, there are two local minima in the free energy corresponding to the composite interface (penetration depth $z \approx 0.3$) and the fully wetted interface (penetration depth $z = 1.0$). Further, the composite interface was observed to have a much lower free energy density as compared to the fully wetted state, thus making it the thermodynamically favored state. However, it is possible to provide enough activation energy to force the droplet to transition to the fully wetted state.[24] This is the idea behind the experiments of Krupenkin et al.,[34] who used electrical current and voltage to provide the activation energy required to reversibly transition between the composite and fully wetted states on the same surface with water. Other calculations on this surface with sinusoidal wrinkles showed that, as θ is reduced to $\theta_c = 118°$, the fully wetted interface has a lower free energy density than the composite interface and becomes the thermodynamically favored state.

Figure 4b shows the Gibbs free energy density calculated for hexadecane ($\theta = 80°$) penetrating into the same sinusoidal surface as in Figure 4a. In this case, only a single global minimum can be observed (at $z = 1.0$), corresponding to the fully wetted interface with $\theta^* = 60°$. Thus, this surface is unable to support a composite superoleophobic interface.

Similar calculations can be performed for the penetration of water (Figure 4c; $\theta = 120°$) and hexadecane (Figure 4d; $\theta = 80°$) into a nonwoven electrospun fiber mat of PMMA and 44.1 wt% fluoroPOSS,[6] shown schematically in Figure 3b. (These electrospun fibers were used to coat the lotus leaf and render it both superhydrophobic and oleophobic, as shown in Figures 1c and 1d.) For water propagating on the electrospun surface, the composite interface is extremely stable and is the thermodynamically favored state, as was the case on the sinusoidal surface in Figure 4a.

For the case of the propagation of hexadecane (Figure 4d), the presence of reentrant curvature allows for the formation of a metastable composite interface (near the penetration depth $z \approx 0.6$), in contrast to the sinusoidal surface discussed earlier. It can also be seen that the overall energy of the surface can be decreased substantially if the surface transitions from the composite to the fully wetted interface; however, there is a significant energy barrier preventing this transition. It is possible to provide the activation energy necessary to induce this transition in a variety of ways, including dropping the liquid droplet from a height or applying external pressure on the drop, leading to a fully wetted interface, as has been observed previously.[6,12,24]

Designing a Robust Composite Interface

The presence of reentrant texture is not a sufficient condition for producing robust superhydrophobic or superoleophobic surfaces. The activation energy required to irreversibly transition from a composite interface to a fully wetted interface is extremely small in many cases.[6] Further, even though a Gibbs free energy approach[20] can reliably predict the existence of a composite interface, its ability to estimate the robustness of the regime is limited,[6] as the analysis typically assumes a locally flat liquid–vapor interface. With actual droplets, having significant internal pressure or being subjected to externally applied pressure, considerable sagging of the liquid–vapor interface can occur. The failure of the composite regime thus typically originates not from the activation energy required to transition between the composite and fully wetted states, but from the imperfections associated with the sagging of the liquid–vapor interface. Hence, the robustness of a composite interface can be significantly lower than the values obtained using Gibbs free-energy calculations.

To provide a relative measure of the pressure required to cause the breakdown of a composite interface, our group at MIT developed a dimensionless robustness parameter H^* (see Reference 6) that parameterizes the sagging of the liquid–vapor interface as a result of pressure imbalance across it (caused by Laplace pressure, external pressure or gravity). H^* compares the maximum pore depth (h_2 in Figure 3b) with the sagging depth of the interface (h_1 in Figure 3b).

Consider the idealized fiber mat surface shown schematically in Figure 3b. Such a surface would fail if the bulging liquid–vapor interface touched the next layer of fibers and the liquid continued to wet the solid substrate. The sagging depth of the liquid–air interface (h_1) in this case is given by

$$h_1 = \kappa^{-1}\{1 - \cos[\sin^{-1}(D\kappa)]\}, \quad (2)$$

where κ is the curvature of the liquid–air interface.[6] Generally

$$\kappa = P / 2\gamma_{lv}, \quad (3)$$

where P is the pressure, and it becomes the inverse of the capillary length

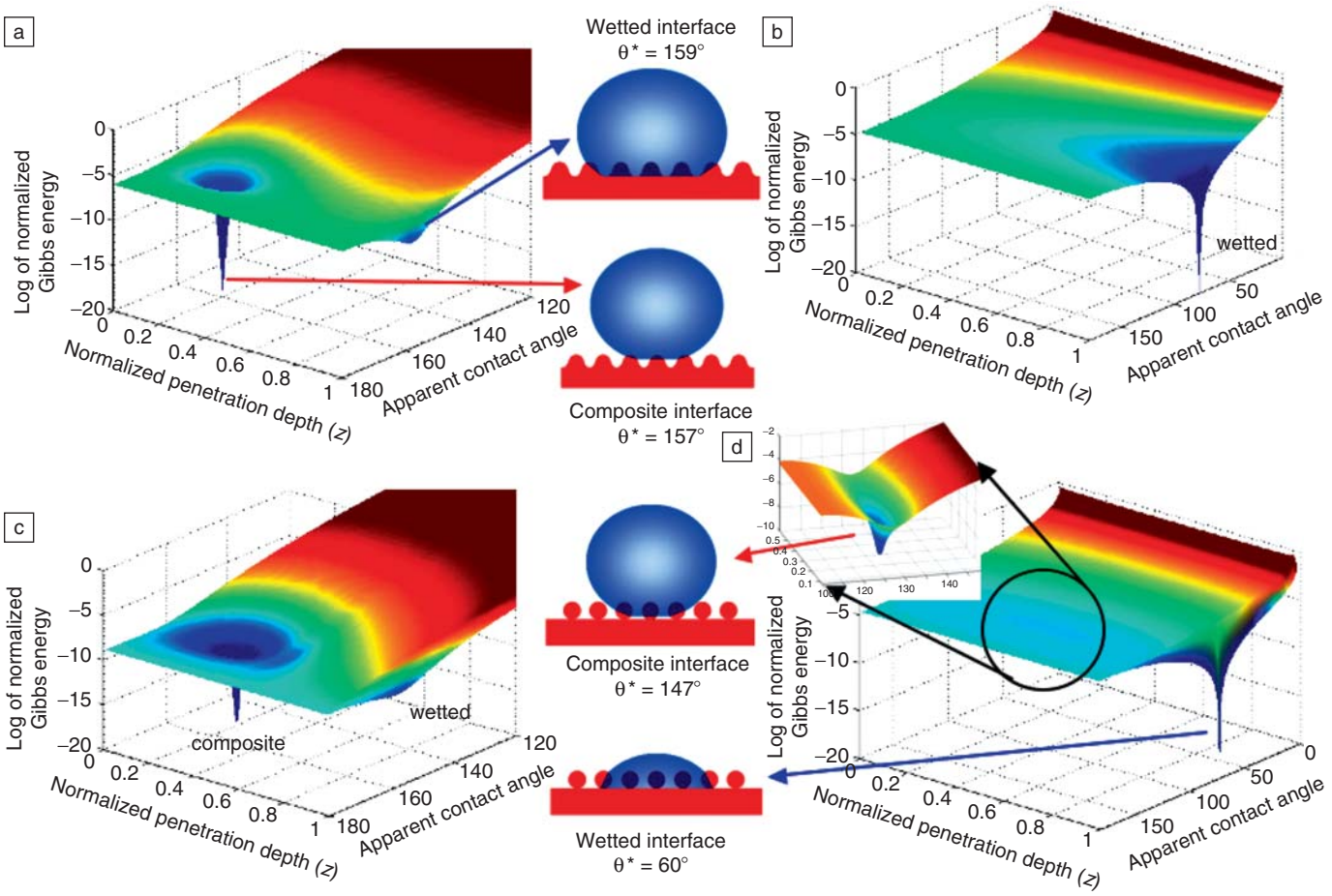

Figure 4. (a) Gibbs free-energy density as a function of apparent contact angle (θ*) and penetration depth (z) for water propagating on a hydrophobic surface (θ = 120°) with sinusoidal wrinkles [given by $y = 0.75\sin^2(\pi x)$]. The two minima in Gibbs energy density at $z \approx 0.3$ and $z \approx 1$ correspond to the composite and the fully wetted interface, respectively. (b) Gibbs free-energy density for hexadecane (θ = 80°) propagating on a surface with sinusoidal wrinkles. Only one minimum in the free energy, corresponding to the fully wetted interface is observed. (c) Gibbs free-energy density as a function of apparent contact angle (θ*) and penetration depth (z) for water (θ = 120°) propagating on a PMMA + 44.1 wt% fluoroPOSS surface. For the calculations, the average fiber radius (R) was taken as 500 nm, and the spacing between fibers (D) was taken to be 1.5 μm. (d) Gibbs free-energy density as a function of apparent contact angle and penetration depth (z) for hexadecane (θ = 80°) propagating on a textured surface of electrospun PMMA + 44.1 wt% fluoroPOSS. The inset shows an enlarged view around $z \approx 0.6$ to illustrate the local minimum in free-energy density for the metastable composite interface.

$$\ell_{cap} = \sqrt{\gamma_{1v} / \rho g} \quad (4)$$

for liquid droplets at equilibrium on a surface under gravity, in the absence of any external pressure. Here, ρ is the liquid density, and g is the acceleration due to gravity.

The system transitions from a composite interface to a fully wetted interface when the sagging height (h_1) becomes equal to the original clearance between the liquid–vapor interface and the next level of fibers (pore depth), $h_2 = R(1 - \cos\theta)$, neglecting any change in the local contact angle due to sagging. When $D << 1 / \kappa \approx \ell_{cap}$ (which is true for most micro or nanoscale textures) $\sin(D\kappa) \approx D\kappa$, giving

$$H^* = h_2 / h_1 \approx 2(1 - \cos\theta)\, R\ell_{cap} / D^2. \quad (5)$$

(See Reference 6 for more detail.)

The robustness parameter for the microhoodoo geometry (Figure 3c) can be similarly calculated to have the form

$$H^* = 2[(1 - \cos\theta)\, R + H]\ \ell_{cap} / D^2. \quad (6)$$

Our group at MIT also defined a second design parameter, D^*, the spacing ratio, that relates the surface texture parameters to the magnitude of the apparent contact angles obtained with any liquid. For a cylindrical geometry, such as the electrospun fibers, Cassie and Baxter[19] showed that the wetted area fraction ϕ_s is a function of the ratio

$$D^* = (R + D) / R. \quad (7)$$

Higher values of the spacing ratio D^* result in lower values of ϕ_s and thus increase the apparent contact angle θ*.

To achieve both extremely high apparent contact angles and robust composite interfaces, the design parameters D^* and H^* must be maximized simultaneously. However, for the case of electrospun fibers, the two design parameters are inherently coupled (see Equations 5 and 7). Increasing the spacing between the fibers (D) leads to higher D^* values but also leads to lower values of H^*, corresponding to more severe sagging of the liquid–air interface. This, in turn, allows for easier liquid penetration through the

structure. For the micro-hoodoo geometry, on the other hand, the spacing ratio takes the new form[6]

$$D^* = \frac{1}{\phi_s} = \left(\frac{W + D}{D}\right)^2. \quad (8)$$

The hoodoo spacing (W) and height (H) can be varied independently (see Figure 3c), so that the spacing ratio (D^*) and the robustness parameter (H^*) can easily be decoupled, thereby giving both high apparent contact angles and a highly robust composite interface on the hoodoo surface, at the same time.

These design parameters provide a mechanism for the rational design of surfaces that are able to support super-repellency, with both high apparent contact angles and a robust composite interface, coupled with low contact-angle hysteresis. Further, they also provide a tool to rank various superhydrophobic or superoleophobic surfaces presented in the literature. Figure 5 shows a plot of the robustness parameter (H^*) as a function of the spacing ratio (D^*) for octane droplets on various natural and artificial surfaces discussed in the literature. More details for each surface, including the values of the apparent contact angles with water and octane, and our estimates of their corresponding dimensionless design parameters are listed in Table I.

Summary

The formation of superhydrophobic or superoleophobic surfaces requires the establishment of a composite interface (enabling the local trapping of air) underneath liquid droplets on a textured surface. It has recently been observed that

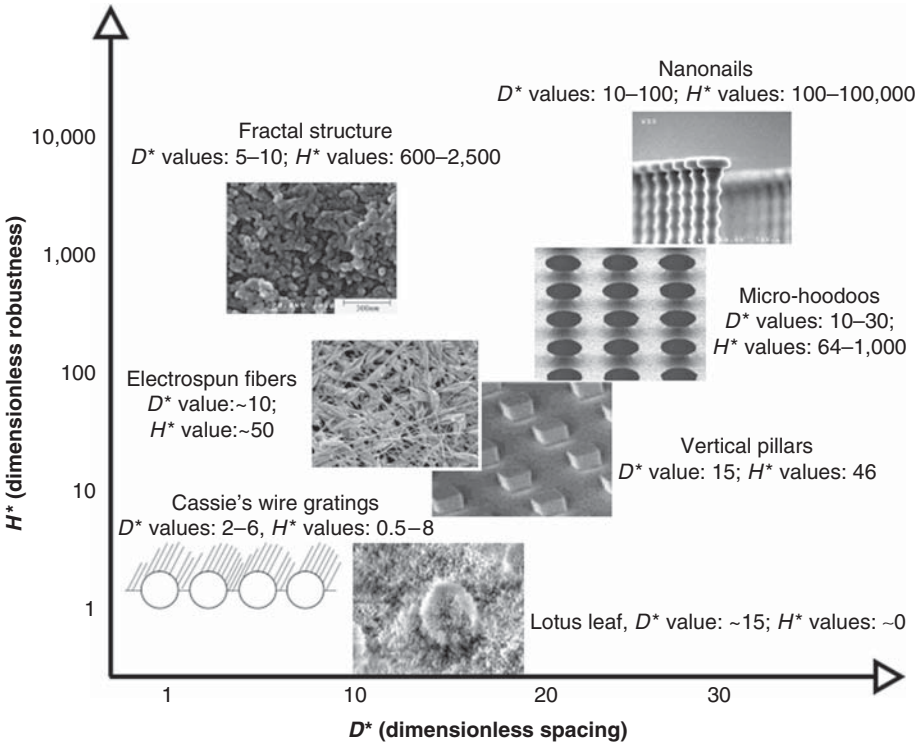

Figure 5. Plot of the robustness parameter (H^*) as a function of the spacing ratio (D^*) for droplets of octane (surface tension γ_{lv} = 21.6 mN/m) on various natural and artificial surfaces presented in the literature. More details for each surface, including values of the apparent contact angles for water and octane and corresponding design parameters are listed in Table I. For low-surface-tension liquids, only surface textures for which the D^* and H^* values can be controlled independently (such as micro-hoodoos or nanonails) show both high apparent contact angles and robustness of the composite interface (as evidenced by a high value for H^*) at the same time. The fractal structure image is reproduced with permission from Reference 8 (Copyright 1997 Wiley-VCH). The nanonail image is reproduced with permission from Reference 10 (Copyright 2008 ACS.) Images of the electrospun fibers, micro-hoodoos, and the lotus leaf are reproduced with permission from Reference 6 (Copyright 2007 AAAS.) The image of the vertical pillars is reproduced with permission from Reference 23 (Copyright 2003 ACS.) The schematic for Cassie's wire gratings is based on the schematic shown in Reference 19.

Table I: Values of the Apparent Contact Angles (θ*) with Water and Octane and Corresponding Values of the Robustness Parameter H^* for Various Natural and Artificial Surfaces Discussed in the Literature.

	Water			Octane		
	θ* (deg)	H^*	θ – ψ[a] (deg)	θ* (deg)	H^*	θ – ψ[a] (deg)
Vertical pillars[23]	~160	~70	30	0	~50	–30
Fractal structure[8 b]	~165	740–3,800	75	0	600–2,500	0
Cassie's wire gratings[19]	~150	3.4–34	105	NA[d]	0.5–8	45
Electrospun fiber surface[6]	~165	~210	120	~140	~50	60
Lotus leaf[c]	~155	~180	~15	0	~0	NA[d]
Micro-hoodoos[6]	~165	95–1,500	120	140–165	64–1,000	60
Nanonails[10]	~150	150–150,000	120	130–150	100–100,000	60

[a]Any liquid for which θ – ψ < 0° will immediately yield a fully wetted interface.

[b]The reentrant angle ψ is hard to measure on randomly shaped textures. On these fractal-like structures, ψ is expected to be ~45° as octane penetrates into the surface texture.

[c]The geometry of the lotus leaf has been estimated through the inspection of various published scanning electron microscopy (SEM) images and is possibly prone to error.

[d]Not available.

many natural and synthetic surfaces are able to support such composite interfaces with various liquids even though the equilibrium contact angles for the surface material are significantly less than 90°. In this article, we have described how this unexpected observance is a direct consequence of the presence of reentrant surface texture, which leads to the formation of a metastable composite interface even with extremely low surface tension liquids such as various alkanes. We have also discussed two dimensionless design parameters, D^* and H^*, which, through the independent control of the surface chemical and topographic features, allow for the development of textured surfaces that can support both an extremely robust composite interface and high contact angles with any liquid.

Acknowledgments

Financial support from the U.S. Air Force Research Laboratory under contract No. FA9300-06M-T015 and the U.S. Air Force Office of Scientific Research under contract No. FA9550-07-1-0272 is gratefully acknowledged. Additional student support was provided by the National Science Foundation Nanoscale Interdisciplinary Research Team on Nanoscale Wetting (contract No. DMR-0303916). We also wish to acknowledge support from the MIT Materials Research Science and Engineering Center through National Science Foundation Award DMR-02-13282.

References

1. Y. Yu, Z.H. Zhao, Q.S. Zheng, *Langmuir* **23** (15), 8212 (2007).
2. M. Callies, D. Quéré, *Soft Mater*. **1** (1), 55 (2005).
3. L. Cao, H.H. Hu, D. Gao, *Langmuir* **23** (8), 4310 (2007).
4. A. Otten, S. Herminghaus, *Langmuir* **20** (6), 2405 (2004).
5. W. Chen, A.Y. Fadeev, M.C. Hsieh, D. Oner, J. Youngblood, T.J. McCarthy, *Langmuir* **15** (10), 3395 (1999).
6. A. Tuteja, W. Choi, M.L. Ma, J.M. Mabry, S.A. Mazzella, G.C. Rutledge, G.H. McKinley, R.E. Cohen, *Science* **318** (5856), 1618 (2007).
7. W.A. Zisman, Relation of the equilibrium contact angle to liquid and solid construction. In *Contact Angle, Wettability and Adhesion, ACS Advances in Chemistry Series* (American Chemical Society: Washington, DC, 1964), vol. 43, pp. 1–51.
8. K. Tsujii, T. Yamamoto, T. Onda, S. Shibuichi, *Angew. Chem., Int. Ed. Engl*. **36** (9), 1011 (1997).
9. S. Shibuichi, T. Yamamoto, T. Onda, K. Tsujii, *J. Colloid Interface Sci*. **208** (1), 287 (1998).
10. A. Ahuja, J.A. Taylor, V. Lifton, A.A. Sidorenko, T.R. Salamon, E.J. Lobaton, P. Kolodner, T.N. Krupenkin, *Langmuir* **24** (1), 9 (2008).
11. S.R. Coulson, I.S. Woodward, J.P.S. Badyal, S.A. Brewer, C. Willis, *Chem. Mater*. **12** (7), 2031 (2000).
12. S. Herminghaus, *Europhys. Lett*. **52** (2), 165 (2000).
13. N.J. Shirtcliffe, G. McHale, M.I. Newton, C.C. Perry, B.F. Pyatt, *Appl. Phys. Lett*. 89 (10), 104106 (2006).
14. L. Zhai, F.C. Cebeci, R.E. Cohen, M.F. Rubner, *Nano Lett*. **4** (7), 1349 (2004).
15. The submerged superhydrophobic surface acts like a mirror because of the total internal reflection of light caused by the entrainment of the thin layer of air between the superhydrophobic surface and water.
16. L. Zhai, M.C. Berg, F.C. Cebeci, Y. Kim, J.M. Milwid, M.F. Rubner, R.E. Cohen, *Nano Lett*. **6** (6), 1213 (2006).
17. F.C. Cebeci, Z. Wu, L. Zhai, R.E. Cohen, M.F. Rubner, *Langmuir* **22** (6), 2856 (2006).
18. R.N. Wenzel, *Ind. Eng. Chem*. **28**, 988 (1936).
19. A.B.D. Cassie, S. Baxter, *Trans. Faraday Soc*. **40**, 546 (1944).
20. A. Marmur, *Langmuir* **19** (20), 8343 (2003).
21. M. Nosonovsky, *Langmuir* **23** (6), 3157 (2007).
22. R.E. Johnson, R.H. Dettre, Contact angle hysteresis. In *Contact Angle, Wettability and Adhesion, ACS Advances in Chemistry Series* (American Chemical Society: Washington, DC, 1964), vol. 43, pp. 112–135.
23. N.A. Patankar, *Langmuir* **19** (4), 1249 (2003).
24. A. Lafuma, D. Quéré, *Nat. Mater*. **2** (7), 457 (2003).
25. B. He, N.A. Patankar, J. Lee, *Langmuir* **19** (12), 4999 (2003).
26. L. Barbieri, E. Wagner, P. Hoffmann, *Langmuir* **23** (4), 1723 (2007).
27. J. Bico, U. Thiele, D. Quéré, *Colloid Surf. A* **206**, 41 (2002).
28. Y.-T. Cheng, D.E. Rodak, *Appl. Phys. Lett*. **86** (14), 144101 (2005).
29. J.-L. Liu, X.-Q. Feng, G. Wang, S.-W. Yu, *J. Phys.: Condens. Matter* **19** (35), 356002 (2007).
30. C.W. Extrand, *Langmuir* **18** (21), 7991 (2002).
31. D.H. Reneker, A.L. Yarin, H. Fong, S. Koombhongse, *J. Appl. Phys*. **87** (9), 4531 (2000).
32. M. Ma, R.M. Hill, J.L. Lowery, S.V. Fridrikh, G.C. Rutledge, *Langmuir* **21** (12), 5549 (2005).
33. M. Ma, M. Gupta, Z. Li, L. Zhai, K.K. Gleason, R.E. Cohen, M.F. Rubner, G.C. Rutledge, *Adv. Mater*. **19** (2), 255 (2007).
34. T.N. Krupenkin, J.A. Taylor, E.N. Wang, P. Kolodner, M. Hodes, T.R. Salamon, *Langmuir* **23** (18), 9128 (2007). □